User-Centric MIMO Techniques for Indoor Visible Light Communication Systems

Chen Chen , *Member, IEEE*, Helin Yang , Pengfei Du , Wen-De Zhong, *Senior Member, IEEE*, Arokiaswami Alphones, *Senior Member, IEEE*, Yanbing Yang , and Xiong Deng

Abstract—Multiple-input multiple-output (MIMO) is a promising technology to efficiently improve the achievable rate of white light-emitting diodes (LEDs) enabled visible light communication (VLC) systems. Nevertheless, for conventional MIMO techniques such as spatial diversity (SD) and spatial multiplexing (SMP), the working mode of each LED transmitter is independent of users' spatial positions. In this article, we propose and investigate three user-centric MIMO techniques, including SD/SMP switching, adaptive SMP (aSMP), and SD-aided aSMP (SD-aSMP), for achievable rate improvement of indoor MIMO-VLC systems, by exploiting users' spatial positions as a new degree of diversity. The analytical and simulation results show that the achievable rate of a 4 × 4 MIMO-VLC system in a typical indoor environment can be significantly improved by applying the user-centric MIMO techniques compared with the conventional ones. More specifically, SD/SMP switching can enjoy both high diversity gain of SD and high multiplexing gain of SMP at different signal-to-noise ratio (SNR) regions, while aSMP mitigates the adverse effect of noise amplification in conventional SMP and SD-aSMP can benefit from additional diversity gain. Furthermore, we also show that the proposed user-centric MIMO techniques outperform conventional MIMO techniques under the condition of only slightly increased computational complexity with limited feedback information.

Index Terms—Multiple-input multiple-output (MIMO), spatial diversity (SD), spatial multiplexing (SMP), visible light communication (VLC), user-centric design.

I. INTRODUCTION

HITE light-emitting diodes (LEDs) are anticipated to replace conventional incandescent and fluorescent lamps for indoor illumination in the near future, due to their inherent

Manuscript received March 26, 2019; revised September 20, 2019 and December 19, 2019; accepted December 19, 2019. Date of publication January 14, 2020; date of current version September 2, 2020. This work was supported by the National Natural Science Foundation of China under Grant 61901065. (Corresponding author: Chen Chen.)

- C. Chen is with the School of Microelectronics and Communication Engineering, Chongqing University, Chongqing 400044, China (e-mail: c.chen@cqu.edu.cn).
- H. Yang, W.-D. Zhong, and A. Alphones are with the School of Electrical and Electronic Engineering, Nanyang Technological University, Singapore 639798 (e-mail: hyang013@e.ntu.edu.sg; ewdzhong@ntu.edu.sg; ealphones@ntu.edu.sg).
- P. Du is with the A*STAR's Singapore Institute of Manufacturing Technology, Singapore 138634 (e-mail: du_pengfei@simtech.a-star.edu.sg).
- Y. Yang is with the College of Computer Science, Sichuan University, Chengdu 610065, China (e-mail: yangyanbing@scu.edu.cn).
- X. Deng is with the Department of Electrical Engineering, Eindhoven University of Technology (TU/e), Flux Building 5600 MB Eindhoven, Netherlands (e-mail: x.deng@tue.nl).

Digital Object Identifier 10.1109/JSYST.2019.2961696

advantages such as high radiative efficiency, long lifetime, high tolerance against humidity, limited heat generation, low cost, and small size [1]. In recent years, white LEDs-enabled visible light communication (VLC) has been considered as a promising complementary technology to traditional radio-frequency (RF) technologies in indoor environments [2]. In typical indoor VLC systems, the LEDs serve a dual-function of both illumination and wireless communication [3]. Compared with traditional RF technologies such as Wi-Fi, VLC (also known as Li-Fi [4]) enjoys many exiting advantages such as huge and unregulated spectrum, potentially high data rate, low-cost front-ends, and no electromagnetic interference [5]. Although white LEDs-based VLC reveals great potential for future green and high-speed indoor wireless communications, there are still many critical issues that need to be addressed. In particular, since the white LEDs are mainly designed for the purpose of efficient lighting, the switching speed (i.e., the modulation bandwidth) of commercial off-the-shelf (COTS) white LEDs¹ is relatively slow [6]. It was reported in [7] that the 3-dB modulation bandwidth of a typical COTS white LED is usually only about several MHz. As a result, the practically achievable rate of an indoor VLC system using COTS white LEDs is very limited.

So far, many techniques have been proposed for achievable rate improvement of VLC systems. In [8] and [9], micro LEDs have been utilized to increase the available 3-dB modulation bandwidth to 100 MHz and more. In [7], [10], and [11], various frequency domain equalization techniques have been applied to extend the modulation bandwidth of COTS white LEDs. In [12] and [13], advanced modulation schemes such as orthogonal frequency division multiplexing (OFDM) and carrierless amplitude and phase modulation using high-order quadrature amplitude modulation constellations have been employed to improve the spectral efficiency. In [14]–[16], spectral-efficient multiple access schemes such as nonorthogonal multiple access have been adopted to boost the overall system capacity. In [17] and [18], multiple-input multiple-output (MIMO) concepts have been introduced to achieve substantial diversity or multiplexing gain. Moreover, the combination of several different techniques have also been considered in VLC systems [19], [20].

Among them, MIMO is a very efficient and natural way to improve the achievable rate of VLC systems using COTS white LEDs, which exploits the existing LED fixtures in the

¹COTS white LEDs are widely adopted for general indoor lighting due to their advantages of high energy efficiency, long lifetime, and low cost.

1937-9234 © 2020 IEEE. Personal use is permitted, but republication/redistribution requires IEEE permission. See https://www.ieee.org/publications/rights/index.html for more information.

ceiling of a typical indoor environment [21]. To date, many transmission schemes have been considered in indoor MIMO-VLC systems, such as spatial diversity (SD), spatial multiplexing (SMP), and spatial modulation (SM) [21]-[23]. In typical indoor environments, the path difference between the multiple transmitter-receiver links is very small and, hence, the temporal delay between the multiple links is negligible [21]. As a result, SD is a simple and effective way to achieve diversity gain in indoor VLC systems. SMP is another widely applied MIMO technique, which can provide certain multiplexing gain and, hence, improve the system capacity [22]. Nevertheless, due to line-of-sight (LOS) transmission and small detector spacing, SMP-VLC systems suffer from high channel correlation, which limits the achievable multiplexing gain. Many schemes have been reported in literature to improve the performance of SMP-VLC systems, such as angle diversity receivers and imaging receivers [24]–[26], transmitter power imbalance and link blockage [21], and non-Hermitian symmetry OFDM modulation [27], [28]. Moreover, transmitter-side precoding has also been applied in SMP-VLC systems in order to obtain parallel channels [29], [30]. However, practical implementation of precoding in VLC systems might be challenging due to the limited dynamic range and the severe nonlinearity of COTS white LEDs [31]. SM technique is a combination of MIMO and digital modulation, where only one LED is activated to transmit signal at any time and additional bits can be transmitted by selecting the index of the activated LED [32]. However, to achieve high rate, the number of transmitters (i.e., LEDs) has to be exponentially increased [33], which might be impractical in indoor environments. For all the above-mentioned MIMO techniques, the working mode of each LED transmitter is independent of users' spatial positions in the MIMO-VLC system.

It has been shown in [34] and [35] that conventional SD achieves high rate only in the small signal-to-noise ratio (SNR) region while conventional SMP outperforms SD only in the large SNR region, and, hence, there are no MIMO techniques that can achieve high rate in both small and large SNR regions. Inspired by the user-centric quality-of-experience optimization and scheduling of multicolor LEDs in VLC systems [36], in this article, we introduce the concept of user-centric MIMO from a user-centric perspective to improve the achievable rate of MIMO-VLC systems over a wide SNR region. Compared with conventional MIMO techniques, the proposed user-centric MIMO concept is developed by fully exploiting users' spatial positions as a new degree of diversity. Three user-centric MIMO techniques are proposed, including SD/SMP switching, adaptive SMP (aSMP), and SD-aided aSMP (SD-aSMP). Actually, SD/SMP switching is not a completely new technique, which has been previously studied to improve the link reliability against shadowing [34] and to adapt to channel correlations [35]. Usercentric aSMP is inspired by the concept of distributed MIMO, which has been applied in VLC systems in [37]. Nevertheless, SD/SMP switching can be viewed a simple and straightforward user-centric MIMO technique, while aSMP is designed in a user-centric manner with a low-complexity heuristic LED subset selection algorithm. Particularly, an SD-aSMP technique is proposed for the first time, which is shown to outperform both SD/SMP switching and aSMP over a wide range of SNRs. In brief, the main contributions of this article are summarized as follows.

- The concept of user-centric MIMO is for the first time proposed for MIMO-VLC systems, which can be realized by treating users' spatial positions as an additional degree of diversity.
- Three user-centric MIMO techniques, including SD/SMP switching, aSMP, and SD-aSMP, are applied in indoor VLC systems and their achievable rates are analytically derived.
- Two algorithms are designed for LED subset selection in aSMP and SD-aSMP.
- 4) Analytical and simulation results are presented to verify the superiority of user-centric MIMO over conventional MIMO techniques in terms of achievable rate.

The rest of this article is organized as follows. In Section II, we describe the mathematical model of a general MIMO-VLC system using intensity modulation/direct detection (IM/DD) with direct current (DC)-biased optical OFDM modulation. The conventional and user-centric MIMO techniques are introduced in Sections III and IV, respectively, where the achievable rates of different MIMO techniques with regard to the transmit SNR are derived. In Section V, we evaluate and compare the achievable rates of both conventional and user-centric MIMO techniques in a typical indoor VLC system through numerical simulations. The receiver-side computational complexity, the uplink feedback requirement, and the feasibility issues to apply user-centric MIMO techniques in practical VLC systems are also analyzed and discussed. Finally, Section VI concludes the article.

Notation: $(\cdot)^T$, $(\cdot)^*$, and $(\cdot)^{\dagger}$ represent the transpose, conjugated transpose, and pseudo inverse of a vector or matrix, respectively. $(\cdot)^{-1}$ denotes the inverse of a matrix. Nonboldface italic letters, lowercase boldface letters, and capital boldface letters represent scalars, vectors, and matrices, respectively.

II. SYSTEM MODEL

In this section, we first describe the mathematical model of a general indoor MIMO-VLC system using IM/DD. The system is assumed to be equipped with N_t LEDs in the ceiling and N_r photodetectors (PDs) at the receiver of an indoor user. Due to the dual-function of LEDs for simultaneous illumination and communication, a dc bias is usually added in addition to the ac signal for each LED so as to achieve data communication without affecting the primary illumination function of LEDs. Hence, the input of each LED is the combination of a dc bias and the ac signal. Let $\mathbf{x} = [x_1, x_2, \dots, x_{N_t}]^T$ be the transmitted electrical ac OFDM signal vector. After free space propagation and dc removal, the received signal vector $\mathbf{y} = [y_1, y_2, \dots, y_{N_r}]^T$ can be expressed by

$$y = Hx + n \tag{1}$$

where **H** denotes the $N_r \times N_t$ MIMO channel matrix and $\mathbf{n} = [n_1, n_2, \dots, n_{N_r}]^T$ is the additive noise vector. In an indoor $N_r \times N_t$ MIMO-VLC system, the channel matrix is

represented by

$$\mathbf{H}_{N_r \times N_t} = \begin{bmatrix} h_{11} & \cdots & h_{1N_t} \\ \vdots & \ddots & \vdots \\ h_{N_r 1} & \cdots & h_{N_r N_t} \end{bmatrix}$$
 (2)

where h_{rt} $(r=1,2,\ldots,N_r;t=1,2,\ldots,N_t)$ denotes the channel gain between the rth PD and the tth LED. Assuming each LED follows a Lambertian radiation pattern and only the LOS component is considered, the LOS channel gain h_{rt} can be calculated by

$$h_{rt} = \frac{(m+1)\rho A}{2\pi d_{rt}^2} \cos^m(\varphi_{rt}) T_s(\theta_{rt}) g(\theta_{rt}) \cos(\theta_{rt})$$
 (3)

where $m=-\ln 2/\ln(\cos(\Psi))$ is the Lambertian emission order and Ψ is the semiangle at half power of LED; ρ and A are the responsivity and the active area of PD, respectively; d_{rt} is the distance between the rth PD and the tth LED; φ_{rt} is the emission angle; θ_{rt} is the incident angle; and $T_s(\theta_{rt})$ and $g(\theta_{rt})$ are the gains of optical filter and lens, respectively. The gain of the optical lens is given by $g(\theta_{rt})=\frac{n_{RI}^2}{\sin^2\Phi}$, where n_{RI} and Φ are the refractive index and the half-angle field-of-view (FOV) of the lens, respectively [38].

It can be observed from (1) that the output signal from each PD is a linear combination of the input signal x_t and the additive noise n_r . To successfully recover the input signals, MIMO demultiplexing at the receiver side is adopted here, since it can be easily implemented in practical VLC systems without the need of adjusting input electrical powers of LEDs. Several MIMO demultiplexing algorithms have been proposed, such as zero-forcing (ZF), minimum mean-square error, and vertical Bell labs layered space-time [22]. Due to its simplicity and low computational complexity, ZF has been widely applied in MIMO-VLC systems [17], [28]. Therefore, we adopt ZF-based MIMO demultiplexing in the following analysis. Based on the obtained channel matrix **H** of the $N_r \times N_t$ MIMO-VLC system, the transmitted OFDM signal vector x can be estimated by multiplying the pseudo inverse of \mathbf{H} , i.e., \mathbf{H}^{\dagger} , with the received signal vector y

$$\hat{\mathbf{x}} = \mathbf{H}^{\dagger} \mathbf{y} = \mathbf{x} + \mathbf{H}^{\dagger} \mathbf{n} \tag{4}$$

where assuming **H** is full-column-rank $(N_r \ge N_t)$, \mathbf{H}^{\dagger} can be calculated by

$$\mathbf{H}^{\dagger} = (\mathbf{H}^* \mathbf{H})^{-1} \mathbf{H}^*. \tag{5}$$

The additive noise in a typical indoor VLC system consists of both the shot and thermal noises [3]. The additive noise n_r is generally modeled as a real-valued zero-mean additive white Gaussian noise with power $P_n = N_0 B$, where N_0 is the noise power spectral density (PSD) and B is the modulation bandwidth.

In indoor VLC systems, the primary function of white LEDs is illumination while communication is only the secondary function. The illumination performance at a specific position of an indoor environment is usually described by the horizontal illuminance. According to [39], the horizontal illuminance can

be defined as follows:

$$E_h = \sum_{t=1}^{N_t} \frac{I_0 \cos^m(\varphi_{rt}) \cos(\theta_{rt})}{d_{rt}^2} \tag{6}$$

where I_0 is the maximum luminous intensity of each LED.

In this article, we analyze and compare the achievable rates of different MIMO techniques in an indoor VLC system. In order to ensure a fair comparison of different MIMO techniques in a typical indoor environment with various geometric setups, we investigate the achievable rates of different MIMO techniques with regard to the SNR at the transmitter side, i.e., transmit SNR [21]. Assuming that the electrical power of the OFDM signals modulated to the activated LEDs is P_s , the transmit SNR can be defined as $\gamma_{\rm tx} = \frac{P_s}{P_o}$.

III. CONVENTIONAL MIMO TECHNIQUES

Two conventional MIMO techniques including SD and SMP are introduced for indoor VLC systems in this section. We first derive the analytical SNRs of SD and SMP, and then obtain their achievable rates with regard to the transmit SNR.

A. Spatial Diversity

As the simplest one in all conventional MIMO techniques, SD is an effective way to achieve transmitter diversity in VLC systems. In SD, all the LEDs transmit the same data stream, i.e., $x_1=x_2=\cdots=x_{N_t}=x_{\rm SD}$, and, hence, MIMO demultiplexing is not required in an SD-VLC system [21]. According to (1), the output signal from the rth PD in the $N_r \times N_t$ SD-VLC system can be represented by

$$y_{r,SD} = \sum_{t=1}^{N_t} h_{rt} x_{SD} + n_r$$
 (7)

where h_{rt} is the channel gain between the rth PD and the tth LED, and n_r is the additive noise of the rth PD. Based on (7), the SNR of the output signal of the rth PD in the $N_r \times N_t$ SD-VLC system is calculated by

$$\gamma_{r,SD} = \frac{\left(\sum_{t=1}^{N_t} h_{rt}\right)^2 P_s}{P_n} = \left(\sum_{t=1}^{N_t} h_{rt}\right)^2 \gamma_{tx}.$$
(8)

Because the output signals of all the PDs contain the same OFDM signal, diversity combining can be used to obtain a final output. Here, maximum-ratio combining (MRC) is adopted due to its superior SNR performance [21]. Using MRC, the output signal from the rth PD is multiplied by a weight $\alpha_r = \gamma_{r,\mathrm{SD}}$ and subsequently the final output signal is obtained by combining all the weighted signals together

$$y_{SD} = \sum_{r=1}^{N_r} \alpha_r y_{r,SD}$$

$$= \sum_{r=1}^{N_r} \left(\alpha_r \sum_{t=1}^{N_t} h_{rt} x_{SD} \right) + \sum_{r=1}^{N_r} \left(\alpha_r n_r \right). \tag{9}$$

Based on (9), the SNR of the combined signal is given by

$$\gamma_{\text{SD}} = \frac{\left(\sum_{r=1}^{N_r} \left(\alpha_r \sum_{t=1}^{N_t} h_{rt}\right)\right)^2 P_s}{\sum_{r=1}^{N_r} \alpha_r^2 P_n}.$$
 (10)

Substitute $\alpha_r = \gamma_{r, \mathrm{SD}}$ into (10) and, thus, we can obtain [40]

$$\gamma_{\rm SD} = \sum_{r=1}^{N_r} \gamma_{r,\rm SD} = \sum_{r=1}^{N_r} \left(\sum_{t=1}^{N_t} h_{rt}\right)^2 \gamma_{\rm tx}.$$
(11)

In this article, we adopt OFDM modulation in the $N_r \times N_t$ MIMO-VLC system, where dc biases are added and Hermitian symmetry constraint is imposed so as to obtain real-valued non-negative LED-compatible OFDM signals [28]. Following (11), the achievable rate, i.e., spectral efficiency (bit/s/Hz), of the $N_r \times N_t$ SD-VLC system can be obtained by

$$R_{SD} = \frac{1}{2} \log_2(1 + \gamma_{SD})$$

$$= \frac{1}{2} \log_2\left(1 + \sum_{r=1}^{N_r} \left(\sum_{t=1}^{N_t} h_{rt}\right)^2 \gamma_{tx}\right)$$
(12)

where the scaling factor $\frac{1}{2}$ is due to the Hermitian symmetry constraint in OFDM modulation.

B. Spatial Multiplexing

SMP is another widely used MIMO technique in indoor VLC systems. When applying SMP, different LEDs simultaneously transmit independent data streams and MIMO demultiplexing is usually required at the receiver side [22].

According to (4) and (5), the estimate of the tth data stream $x_{t, \mathrm{SMP}}$ in the $N_r \times N_t$ SMP-VLC system is given by

$$\hat{x}_{t,\text{SMP}} = x_{t,\text{SMP}} + \sum_{r=1}^{N_r} \tilde{h}_{tr} n_r$$
 (13)

where \tilde{h}_{tr} is the element in the tth row and the rth column of \mathbf{H}^{\dagger} . Based on (13), the SNR of $\hat{x}_{t,\mathrm{SMP}}$ is calculated by

$$\gamma_{t,\text{SMP}} = \frac{P_s}{\sum_{r=1}^{N_r} \tilde{h}_{tr}^2 P_n} = \frac{\gamma_{\text{tx}}}{\sum_{r=1}^{N_r} \tilde{h}_{tr}^2}.$$
 (14)

The overall achievable rate of the $N_r \times N_t$ SMP-VLC system can be obtained by the sum of the achievable rates of all the independent data streams

$$R_{\text{SMP}} = \sum_{t=1}^{N_t} \frac{1}{2} \log_2(1 + \gamma_{t,\text{SMP}})$$

$$= \frac{1}{2} \sum_{t=1}^{N_t} \log_2\left(1 + \frac{\gamma_{\text{tx}}}{\sum_{r=1}^{N_r} \tilde{h}_{tr}^2}\right). \tag{15}$$

IV. USER-CENTRIC MIMO TECHNIQUES

In conventional MIMO techniques such as SD and SMP, the transmission mode is always fixed, which is independent of the channel conditions of a user.² However, by considering different channel conditions of a user at different spatial positions, the transmission mode of a MIMO system can be designed in a user-centric manner, which can be viewed as a new degree of diversity to improve the achievable rate of conventional MIMO-VLC systems. In this section, we propose and investigate three user-centric MIMO techniques for indoor VLC systems, including SD/SMP switching, aSMP, and SD-aSMP. The SNRs of these three user-centric MIMO techniques are analyzed and their achievable rates with regard to the transmit SNR are further derived.

A. SD/SMP Switching

The first proposed user-centric MIMO technique is SD/SMP switching, in which the MIMO mode is dynamically switched between SD and SMP. When the MIMO-VLC system is in the SD mode, all the LEDs are utilized to transmit the same data stream, as discussed in Section III-A. When the MIMO-VLC system is in the SMP mode, different LEDs are used to transmit different data streams, as introduced in Section III-B.

In SD/SMP switching, the two modes (i.e., SD and SMP) are dynamically switched to achieve a higher rate. As a result, following (12) and (15), the achievable rate of an $N_r \times N_t$ MIMO-VLC system applying SD/SMP switching is given by

$$R_{\rm SD/SMP} = \begin{cases} R_{\rm SD}, & \text{if } R_{\rm SD} \ge R_{\rm SMP} \\ R_{\rm SMP}, & \text{if } R_{\rm SD} < R_{\rm SMP}. \end{cases}$$
 (16)

B. Adaptive Spatial Multiplexing

In conventional SMP, all the LEDs are activated to transmit signals, regardless the users' spatial positions. By exploiting the users' spatial positions as a new degree of diversity, we propose a user-centric aSMP technique for indoor VLC systems to improve the achievable rate. In aSMP, only a subset of the LEDs are activated to transmit independent data streams, while the others are only used for illumination.

To perform aSMP, we rewrite the channel matrix H given in (2) as

$$\mathbf{H}_{N_{-} \times N_{+}} = [\mathbf{h}_{1}, \mathbf{h}_{2}, \dots, \mathbf{h}_{N_{+}}] \tag{17}$$

where the vector element $\mathbf{h}_t = [h_{1t}, h_{2t}, \dots, h_{N_r t}]^T$ of the channel matrix \mathbf{H} is corresponding to the tth LED. Assuming totally k $(1 \le k \le N_t)$ LEDs are activated for signal transmission, the dimension of the channel matrix is, then, changed to $N_r \times k$ and the resultant channel matrix \mathbf{L} can be represented by

(15)
$$\mathbf{L}_{N_r \times k} = [\mathbf{l}_1, \mathbf{l}_2, \dots, \mathbf{l}_k] = \begin{bmatrix} l_{11} & \cdots & l_{1k} \\ \vdots & \ddots & \vdots \\ l_{N_r 1} & \cdots & l_{N_r k} \end{bmatrix}.$$
 (18)

²Although CSI is generally utilized for MIMO demultiplexing, it has not yet been adopted to dynamically change the MIMO transmission mode.

Algorithm 1: LED Subset Selection in aSMP.

```
Initialize K = \{1, 2, ..., N_t\}, \mathbf{H}_c = \{\mathbf{h}_1, \mathbf{h}_2, ..., \mathbf{h}_{N_t}\}
        Calculate the mean vector \boldsymbol{\epsilon} = \{\epsilon_1, \epsilon_2, \dots, \epsilon_{N_t}\} of
        \mathbf{H}_c, where \epsilon_t denotes the mean of \mathbf{h}_t
        (t = 1, 2, \dots, N_t)
        Sort \epsilon in the descending order and obtain the
        corresponding index vector \mathbf{q} = \{q_1, q_2, \dots, q_{N_t}\}
        for k = N_t to 2 do
 4:
           if k = N_t then
 5:
             Update \mathbf{L}_c = \mathbf{H}_c, Q_k = K
 6:
 7:
             Obtain L according to L_c
 8:
             Calculate R_{aSMP,k} using (19)
 9:
             Update \mathbf{L}_c = \mathbf{L}_c - \{\mathbf{h}_{q_k}\}, Q_k = Q_k - \{q_k\}
Obtain \mathbf{L} according to \mathbf{L}_c
10:
11:
12:
             Calculate R_{aSMP,k} using (19)
13:
           end if
14:
        end for
15:
        Obtain the index k_{\text{opt}} that maximizes R_{\text{aSMP},k}
        Output the optimal LED subset Q_{k_{out}}
16:
```

Following (15), the overall achievable rate of the VLC system using aSMP with k activated LEDs is obtained by

$$R_{\text{aSMP},k} = \frac{1}{2} \sum_{t=1}^{k} \log_2 \left(1 + \frac{\gamma_{\text{tx}}}{\sum_{r=1}^{N_r} \widetilde{i}_{tr}^2} \right)$$
 (19)

where \widetilde{l}_{tr} is the element in the tth row and the rth column of \mathbf{L}^{\dagger} , i.e., the pseudo inverse of \mathbf{L} .

The key idea of performing aSMP is to select a subset of all the N_t LEDs for signal transmission that maximizes the achievable rate of the VLC system. The detailed procedures of LED subset selection in aSMP are given in Algorithm 1. In the initialization stage, the index vector of all the LEDs in the VLC system is defined by $K = \{1, 2, \dots, N_t\}$ and the channel matrix **H** is rewritten as a combination of its vector elements, i.e., $\mathbf{H}_c =$ $\{\mathbf{h}_1,\mathbf{h}_2,\ldots,\mathbf{h}_{N_t}\}$. The mean vector $\boldsymbol{\epsilon}=\{\epsilon_1,\epsilon_2,\ldots,\epsilon_{N_t}\}$ of \mathbf{H}_c is first calculated, where ϵ_t $(t=1,2,\ldots,N_t)$ denotes the mean of h_t . Subsequently, ϵ is sorted in the descending order and the corresponding index vector $\mathbf{q} = \{q_1, q_2, \dots, q_{N_t}\}$ is obtained. The iteration starts from $k = N_t$, where all the LEDs are selected and the corresponding achievable rate $R_{aSMP,k}$ is calculated by using (19). After that, the LED, which is the farthest from the user, is removed from the LED subset Q_k , in order to reduce channel correlation as well as noise amplification. The channel matrix is updated and the achievable rate is, then, calculated using the updated channel matrix accordingly. Following this manner, the LEDs in the subset Q_k are removed one by one until there is only one LED left. Consequently, the maximal achievable rate $R_{aSMP,max}$ of the aSMP-based VLC system can be found and its corresponding index k_{opt} can be used to identify the optimal LED subset $Q_{k_{out}}$.

C. Spatial Diversity-Aided Adaptive Spatial Multiplexing

In aSMP, the number of the activated LEDs for signal transmission might be smaller than the number of all the LEDs, indicating that some of the LEDs are only driven by the dc bias for illumination.³ From the perspective of resource utilization, it can be seen as a waste of resource since these LEDs are already there but not used for the purpose of communication. To fully utilize all the resources, the third user-centric MIMO technique is proposed, which is named SD-aSMP. In user-centric SD-aSMP, all the LEDs are activated to transmit signals and some of the them are used to transmit the same data stream. As a result, SD-aSMP can be considered as a modified version of aSMP, where the deactivated LEDs in aSMP are reactivated to transmit the same data stream as a specific activated LED, so as to achieve additional diversity gain. Here, we assume that the deactivated LEDs are used to transmit the same data stream as the activated LED, which is the farthest from the user. In this manner, the received power of the signal transmitted by the farthest LED can be efficiently increased due to the additional diversity gain, and, hence, the adverse effect of noise amplification can be further reduced in comparison to aSMP.

We assume that a subset of k LEDs are employed to transmit different data streams and the zth $(1 \le z \le k)$ LED in the subset is the farthest one from the user. Therefore, the corresponding channel matrix of these k LEDs in the subset can be expressed by $\mathbf{W}_{N_r \times k} = [\mathbf{w}_1, \dots, \mathbf{w}_z, \dots, \mathbf{w}_k]$. In addition, the remaining $N_t - k$ LEDs are utilized to transmit the same data stream as the zth LED and the channel matrix with respect to these $N_t - k$ LEDs can be represented by $\mathbf{V}_{N_r \times (N_t - k)} = [\mathbf{v}_1, \mathbf{v}_2, \dots, \mathbf{v}_{N_t - k}]$. Hence, the resultant channel matrix of SD-aSMP is given by

$$\mathbf{F}_{N_r \times k} = \begin{bmatrix} \mathbf{w}_1, \dots, \mathbf{w}_z + \sum_{i=1}^{N_t - k} \mathbf{v}_i, \dots, \mathbf{w}_k \end{bmatrix}. \tag{20}$$

Using ZF-based MIMO demultiplexing, the pseudo inverse \mathbf{F}^{\dagger} of \mathbf{F} can be obtained as per (5). Therefore, based on (19), the overall achievable rate of the VLC system adopting SD-aSMP with k independent data streams is obtained by

$$R_{\text{SD-aSMP},k} = \frac{1}{2} \sum_{t=1}^{k} \log_2 \left(1 + \frac{\gamma_{\text{tx}}}{\sum_{r=1}^{N_r} \tilde{f}_{tr}^2} \right)$$
 (21)

where \widetilde{f}_{tr} is the element in the tth row and the rth column of \mathbf{F}^{\dagger} , i.e., the pseudo inverse of \mathbf{F} . Algorithm 2 shows the detailed procedures of LED subset selection for transmitting different data streams in user-centric SD-aSMP, in which $\mathbf{W}_c = \{\mathbf{w}_1, \mathbf{w}_2, \dots, \mathbf{w}_k\}$ and $\mathbf{V}_c = \{\mathbf{v}_1, \mathbf{v}_2, \dots, \mathbf{v}_{N_t-k}\}$. Consequently, the optimal LED subset $Q_{k_{\mathrm{opt}}}$ can be found for the VLC system using SD-aSMP to achieve the maximal rate $R_{\mathrm{SD-aSMP,max}}$.

³A proper dc bias is generally required by each LED transmitter so as to maintain stable illumination.

Algorithm 2: LED Subset Selection in SD-aSMP. Initialize $K = \{1, 2, ..., N_t\}, \mathbf{H}_c = \{\mathbf{h}_1, \mathbf{h}_2, ..., \mathbf{h}_{N_t}\}$ Calculate the mean vector $\boldsymbol{\epsilon} = \{\epsilon_1, \epsilon_2, \dots, \epsilon_{N_t}\}$ of \mathbf{H}_c , where ϵ_t denotes the mean of \mathbf{h}_t $(t = 1, 2, \dots, N_t)$ Sort ϵ in the descending order and obtain the corresponding index vector $\mathbf{q} = \{q_1, q_2, \dots, q_{N_t}\}$ for $k = N_t$ to 2 do 4: if $k = N_t$ then 5: Update $\mathbf{W}_c = \mathbf{H}_c$, $\mathbf{V}_c = \emptyset$, $Q_k = K$ 6: 7: Update \mathbf{F}_c using (20) 8: Obtain **F** according to \mathbf{F}_c 9: Calculate $R_{\text{SD-aSMP},k}$ using (21) 10: Update $\mathbf{W}_c = \mathbf{W}_c - \{\mathbf{h}_{q_k}\}, \mathbf{V}_c = \mathbf{V}_c + \{\mathbf{h}_{q_k}\},$ 11: $Q_k = Q_k - \{q_k\}$ Update \mathbf{F}_c using (20) 12: 13: Obtain \mathbf{F} according to \mathbf{F}_c Calculate $R_{\text{SD-aSMP},k}$ using (21) 14: 15: end if 16: end for

V. PERFORMANCE EVALUATION AND COMPARISON

Obtain the index k_{opt} that maximizes $R_{\text{SD-aSMP},k}$

Output the optimal LED subset $Q_{k_{\mathrm{opt}}}$

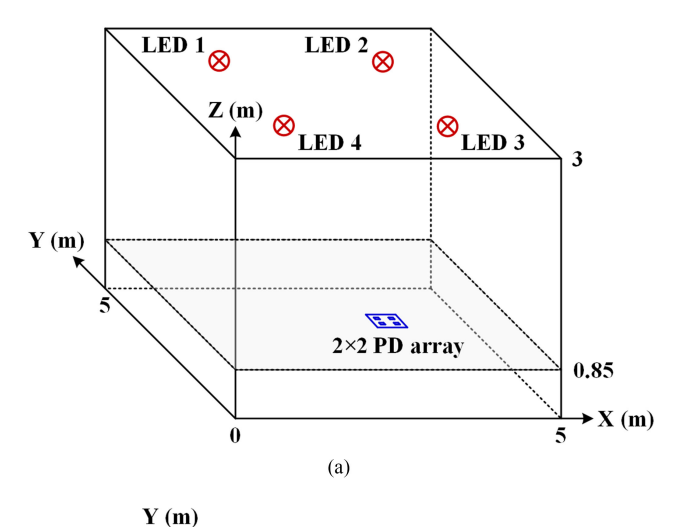
In this section, we evaluate and compare the performance of conventional and user-centric MIMO techniques in a typical indoor VLC system through numerical simulations.

A. Simulation Setup

17:

18:

In our simulations, we use MATLAB as the simulator and consider a 4 × 4 MIMO-VLC system in an indoor environment with a dimension of 5 m \times 5 m \times 3 m. The geometric setup of the 4×4 MIMO-VLC system is shown in Fig. 1(a), where X (m), Y (m), and Z (m) indicate the three axes of the 3-D coordinate system with unit meter, respectively. Four LEDs are mounted in the ceiling and the user equipped with a 2×2 PD array is located within the receiving plane, which is 0.85 m above the floor. The LEDs are oriented downwards to point straight to the receiving plane and the PDs are vertically oriented toward the ceiling. As can be seen from Fig. 1(b), both the LEDs and the PDs are placed in a square grid. The center of the LED array is (2.5, 2.5, and 3 m), i.e., the center of the ceiling, and the spacing between adjacent two LEDs is denoted by d_{LED} . The center of the PD array is determined by the position of the user and the spacing between adjacent two PDs is given by d_{PD} . The key simulation parameters are listed in Table I. The semiangle at half power and the maximum luminous intensity of each LED are 70° and 3000 cd, respectively. The gain of the optical filter is 0.9. The refractive index and the half-angle FOV of the optical lens are 1.5 and 70°, respectively. Each PD has a responsivity of 0.53 A/W and an active area of 1 cm². The modulation bandwidth is set to 20 MHz and the noise PSD is 10^{-22} A^2/Hz . For OFDM modulation, the size of inverse fast Fourier transform (IFFT)



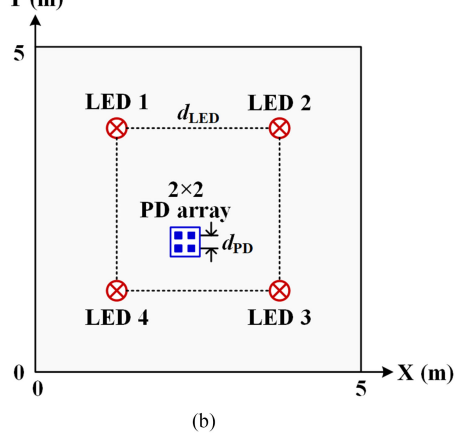


Fig. 1. (a) Geometric setup and (b) top view of the 4×4 MIMO-VLC system.

TABLE I SIMULATION PARAMETERS

Parameter	Value
Room dimension	$5 \text{ m} \times 5 \text{ m} \times 3 \text{ m}$
Height of receiving plane	0.85 m
Semi-angle at half power of LED	70°
Maximum luminous intensity of LED	3000 cd
Gain of optical filter	0.9
Refractive index of optical lens	1.5
Half-angle FOV of optical lens	70°
Responsivity of PD	0.53 A/W
Active area of PD	1 cm^2
Modulation bandwidth	20 MHz
Noise power spectral density	$10^{-22} \text{ A}^2/\text{Hz}$
IFFT/FFT size	128
Number of data subcarriers	63
Constellation	BPSK

and fast Fourier transform (FFT) is 128 and the number of data subcarrier is 63. The constellation of binary phase shift keying (BPSK) is adopted for SNR estimation via the received error vector magnitude value.

B. Achievable Rate

We first investigate the achievable rates of conventional and user-centric MIMO techniques in the indoor 4×4 MIMO-VLC system. Fig. 2 shows the achievable rate versus the transmit SNR

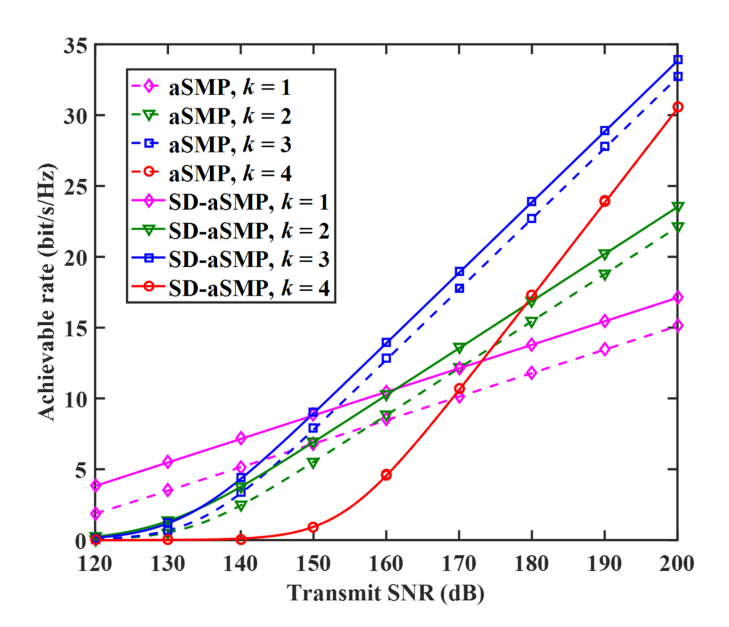


Fig. 2. Achievable rate versus transmit SNR for aSMP and SD-aSMP with different number (k) of independent data streams at the center of the room for $d_{\rm LED}=3$ m and $d_{\rm PD}=20$ cm. Markers show the simulation results and lines give the corresponding analytical results.

for aSMP and SD-aSMP with totally k independent data streams at the center of the receiving plane for LED spacing $d_{\rm LED}=3$ m and PD spacing $d_{\rm PD}=20$ cm. In Fig. 2, the simulation results and the analytical results are given by the markers and the lines, respectively. As can be seen, the simulation results agree well with the analytical predictions.

Applying (2) to this geometric scenario yields the following 4×4 channel matrix:

$$\mathbf{H}_{4\times4} \approx 10^{-6} \begin{bmatrix} 1.992 & 1.760 & 1.567 & 1.760 \\ 1.760 & 1.567 & 1.760 & 1.992 \\ 1.567 & 1.760 & 1.992 & 1.760 \\ 1.760 & 1.992 & 1.760 & 1.567 \end{bmatrix} . \tag{22}$$

It can be seen from (22) that the channel coefficients are on the order of 10^{-6} , which is corresponding to an electrical path loss of about 120 dB at the receiver side. Therefore, in order to evaluate the achievable rates of different MIMO techniques over a wide range of SNRs, the transmit SNR in the evaluation is set in the range between 120 to 200 dB.

When aSMP is employed in the indoor 4×4 MIMO-VLC system, as shown by the dashed lines in Fig. 2, the achievable rates of aSMP are quite different when k takes different values. For aSMP with k=1, only one LED is activated to transmit signal while the other three LEDs are simply used for indoor illumination. As we can see, the achievable rate has nearly a linear relationship with the transmit SNR in the unit of dB. For example, the achievable rate is 10.2 bit/s/Hz when the transmit SNR is 170 dB, which is increased to 11.8 bit/s/Hz when the transmit SNR is 180 dB. However, for aSMP with k=2, 3 and 4, more than one LED is activated to transmit independent data streams and MIMO demultiplexing is usually required, which leads to noise amplification and the reduction of achievable rate. It can be observed that the achievable rate increases slowly with

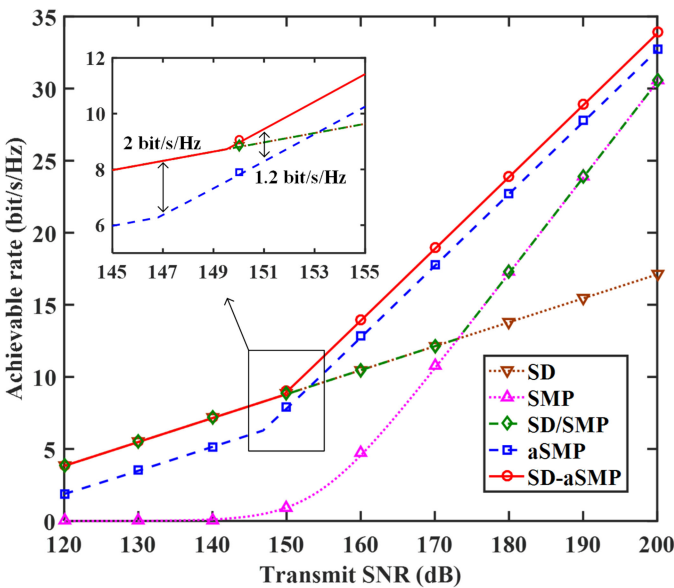


Fig. 3. Achievable rate comparison of SD, SMP, SD/SMP switching (SD/SMP), aSMP and SD-aSMP at the center of the room with $d_{\rm LED}=3$ m and $d_{\rm PD}=20$ cm. Markers show the simulation results and lines give the corresponding analytical results.

the transmit SNR when the transmit SNR is relatively small, showing that the achievable rate is mainly dominated by the adverse effect of noise amplification in the small SNR region. In contrast, when the transmit SNR becomes relatively large, the achievable rate is almost linearly increased with the transmit SNR, suggesting that the achievable rate is mainly dominated by the multiplexing gain in the large SNR region. Furthermore, it can be seen that SD-aSMP achieves higher rate than aSMP for k=1,2 and 3, as depicted by the solid lines in Fig. 2. When k=1, SD-aSMP becomes the conventional SD since all the LEDs are used to transmit the same data stream, which outperforms aSMP due to high diversity gain. In addition, when k=4, both aSMP and SD-aSMP become the conventional SMP.

It is important for us to observe from Fig. 2 that the k value to achieve the maximum rate is different for different transmit SNR conditions. For example, the maximum rate of aSMP is achieved for k=1 when the transmit SNR is in the range between 120 to 146.8 dB. However, when the transmit SNR is larger than 146.8 dB, the k value to achieve the maximum rate of aSMP becomes 3. Similarly, the k value to achieve the maximum rate of SD-aSMP is 1 in the small SNR region and the k value becomes 3 in the large SNR region. The only difference is that the SNR boundary is increased from 146.8 to 149.5 dB. In summary, the achievable rates of both aSMP and SD-aSMP can be maximized by choosing proper k values.

Fig. 3 compares the achievable rate of conventional and user-centric MIMO techniques at the center of the receiving plane with $d_{\rm LED}=3$ m and $d_{\rm PD}=20$ cm. It can also be clearly observed that the obtained simulation results closely match the analytical predictions. As we can see, SMP performs the worst in the small SNR region, which is due to the substantial noise amplification in MIMO demultiplexing. Moreover, SD performs the best in the small SNR region owing to its high diversity gain. With

the increase of the transmit SNR, the achievable rate of SMP increases rapidly due to its high multiplexing gain. The same rate of about 12.6 bit/s/Hz can be achieved by both SD and SMP at a transmit SNR of 173.1 dB, and SMP outperforms SD when the transmit SNR is larger than 173.1 dB.

By adopting user-centric SD/SMP switching, as shown in Fig. 3, the MIMO-VLC system enjoys high diversity gain in the small SNR region and high multiplexing gain in the large SNR region. When applying user-centric aSMP, only an optimal subset of LEDs are selected to transmit independent data streams and, hence, the adverse effect of noise amplification can be mitigated, which leads to a substantial rate improvement compared with SMP. Nevertheless, aSMP performs worse than SD in the small SNR region.⁴ In contrast, user-centric SD-aSMP achieves the best performance among all conventional and user-centric MIMO techniques over both small and large SNR regions. As we can see, SD-aSMP achieves the same rate as SD and SD/SMP switching in the small SNR region, but outperforms aSMP. More specifically, as can be found in the inset of Fig. 3, the achievable rates of SD-aSMP are 2 and 1.2 bit/s/Hz higher than that of aSMP when the transmit SNRs are 147 and 151 dB, respectively. The achievable rate improvement of SD-aSMP in comparison to aSMP is due to the additional diversity gain.

In Figs. 2 and 3, we investigate and compare the achievable rates of conventional and user-centric MIMO techniques at the center of the room. In order to present the overall performance of different MIMO techniques around the entire receiving plane, we further evaluate the achievable rate distributions over the receiving plane in the indoor 4×4 MIMO-VLC system, where the transmit SNR is 180 dB, the LED spacing is 3 m and the PD spacing is 20 cm. Fig. 4(a) and (b) show the achievable rate distributions using conventional SD and SMP, respectively. As we can see, the achievable rate using SD is in the range between 13.6 and 14 bit/s/Hz, while it is between 10.3 and 25.1 bit/s/Hz when using SMP. As a result, the achievable rate distribution of SD is quite flat over the receiving plane, while the maximum rate of SMP is achieved when the user is located at the center and the rate reduces rapidly when the user moves toward the corners. Fig. 4(c) depicts the achievable rate distribution using user-centric SD/SMP switching, where the MIMO-VLC system is in the SMP mode when the user is located near the center of the room and it switches to the SD mode when the user is near the four corners. In contrast, by applying user-centric aSMP, the achievable rate can be significantly improved across the whole room, as shown in Fig. 5(a), which is contributed by exploiting users' spatial positions as a new degree of diversity. Moreover, it can be observed from Fig. 5(b) that the overall achievable rate can be further improved by applying SD-aSMP. Since illumination is the primary function of the LEDs in the indoor MIMO-VLC system, we also evaluate the illumination performance of the system. Fig. 6 illustrates the horizontal illuminance across the receiving plane, where the achievable illuminance is in the range between 680 to 880 lx within the room, which can meet

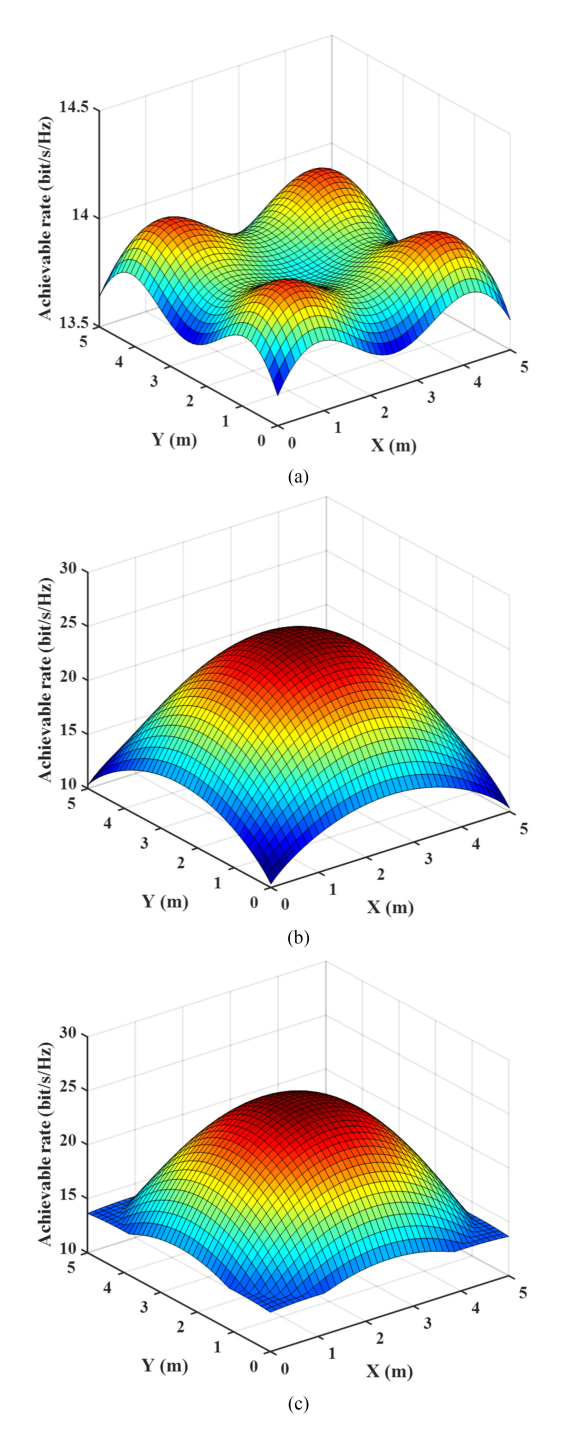


Fig. 4. Achievable rate distribution: (a) SD, (b) SMP, and (c) SD/SMP switching with $\gamma_{\rm tx}=180$ dB, $d_{\rm LED}=3$ m, and $d_{\rm PD}=20$ cm.

the illumination requirements suggested by the European lighting standard [41].

In the above evaluations, we only consider the indoor 4×4 MIMO-VLC system with a specific geometric setup and a fixed transmit SNR. In the following, we analyze the achievable rate performance of the system applying the proposed user-centric MIMO techniques under various transmit SNR conditions and geometric setups. Fig. 7 shows the cumulative distribution function (CDF) plots of the achievable rates using user-centric

⁴This performance gap in the small SNR region is mainly due to the existence of deactivated LED(s) in aSMP.

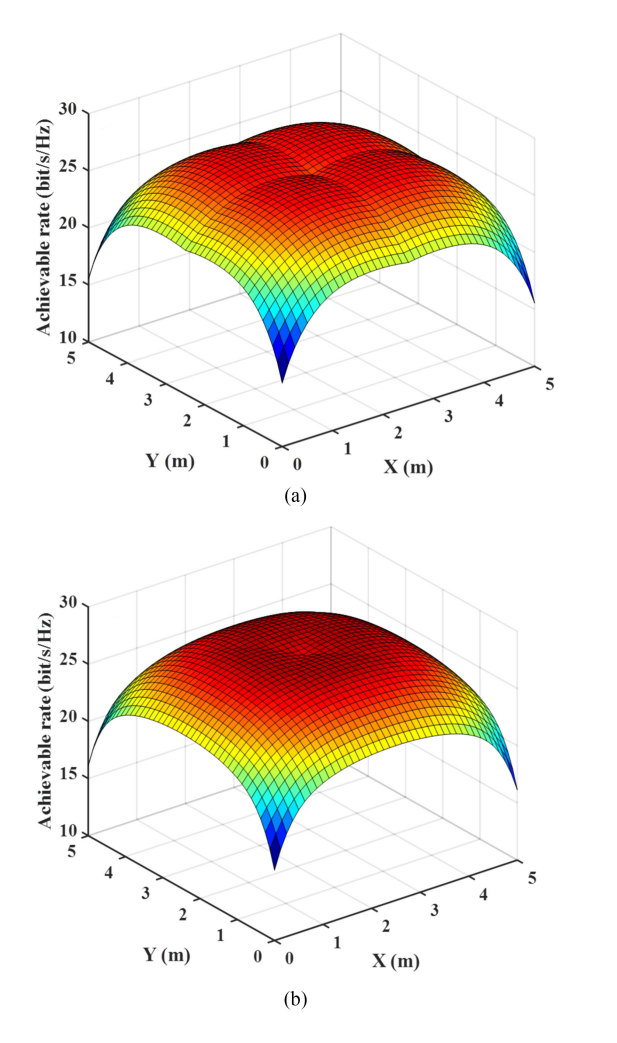


Fig. 5. Achievable rate distribution: (a) aSMP and (b) SD-aSMP with $\gamma_{\rm IX}=180$ dB, $d_{\rm LED}=3$ m, and $d_{\rm PD}=20$ cm.

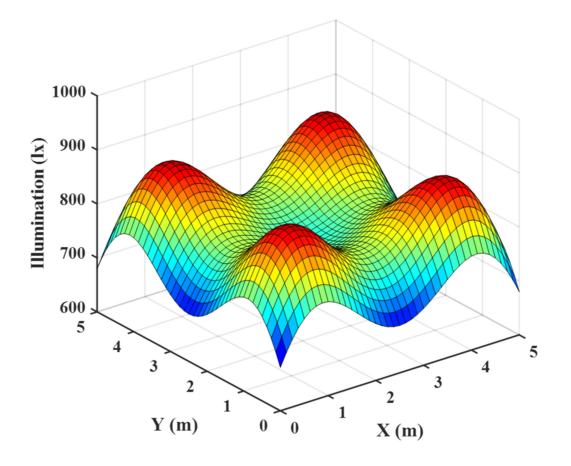


Fig. 6. Illumination distribution over the receiving plane.

SD/SMP switching, aSMP, and SD-aSMP for the LED spacing of 3 m and the PD spacing of 20 cm with two different transmit SNR conditions. It is clear that the achievable rate can be substantially improved when the transmit SNR is increased from 170 to 180 dB, for all the three user-centric MIMO techniques. Taking SD/SMP switching, for example, the minimum

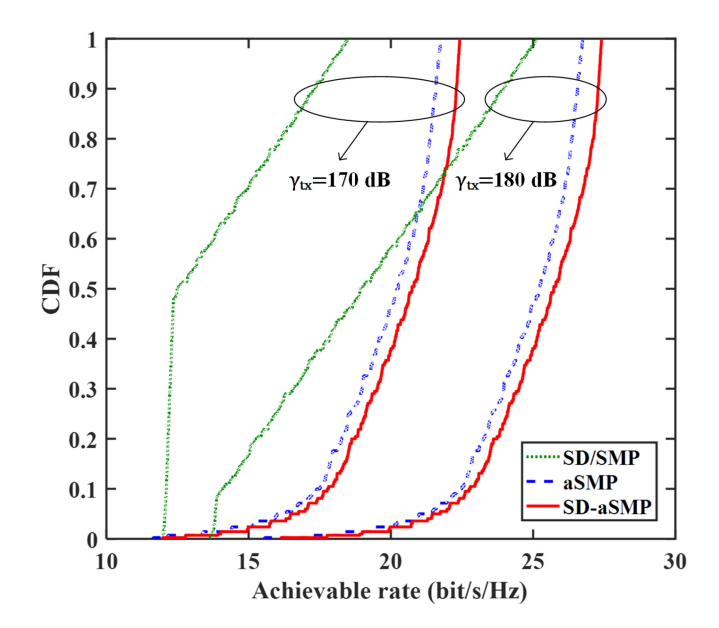


Fig. 7. CDF plot of achievable rate for three user-centric MIMO techniques with $d_{\rm LED}=3$ m, $d_{\rm PD}=20$ cm, and different $\gamma_{\rm tx}$ values. SD/SMP: SD/SMP switching; aSMP: adaptive SMP; SD-aSMP: SD-aided adaptive SMP.

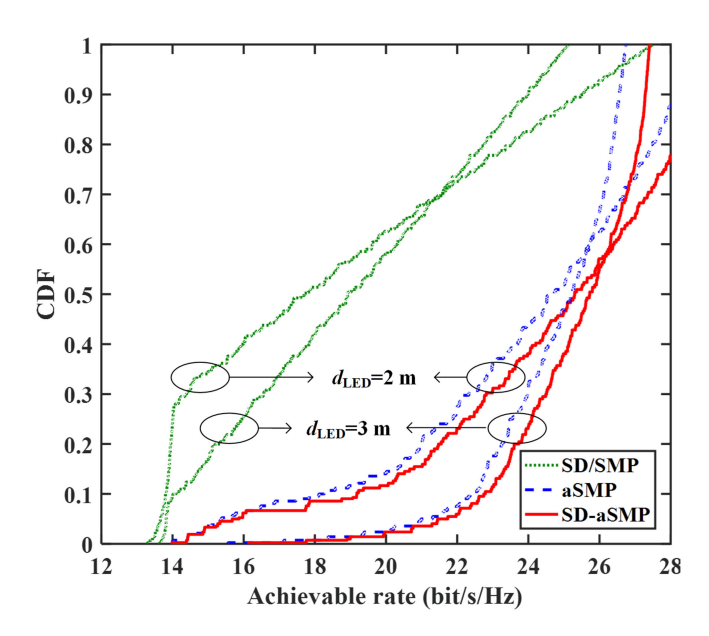


Fig. 8. CDF plot of achievable rate for three user-centric MIMO techniques with $\gamma_{\rm tx}=180~{\rm dB},\,d_{\rm PD}=20~{\rm cm}$ and different $d_{\rm LED}$ values. SD/SMP: SD/SMP switching; aSMP: adaptive SMP; SD-aSMP: SD-aided adaptive SMP.

achievable rate across the whole room is increased from 17.2 to 25.1 bit/s/Hz, indicating an achievable rate improvement of 7.9 bit/s/Hz in corresponding to a 10-dB transmit SNR increase. In Fig. 8, we fix the transmit SNR to 180 dB, set the PD spacing to 20 cm, and vary the LED spacing between 2 and 3 m. As we can see that the minimum achievable rates across the whole room for all the three user-centric MIMO techniques are reduced when the LED spacing is increased from 2 to 3 m, showing that the performance of the 4×4 MIMO-VLC system is largely dependent on the layout of the LED array in the ceiling. Moreover, Fig. 9 compares the achievable rates with different PD

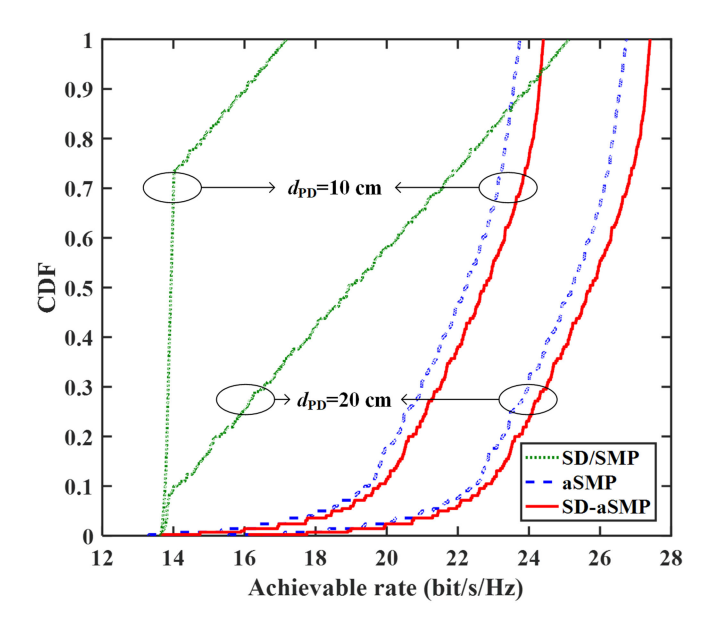


Fig. 9. CDF plot of achievable rate for three user-centric MIMO techniques with $\gamma_{\rm tx}=180~{\rm dB},~d_{\rm LED}=3~{\rm m},$ and different $d_{\rm PD}$ values. SD/SMP: SD/SMP switching; aSMP: adaptive SMP; SD-aSMP: SD-aided adaptive SMP.

spacing with the transmit SNR of 180 dB and the LED spacing of 3 m. It can be observed that the minimum achievable rates across the whole room for all the three user-centric MIMO techniques are greatly improved when the PD spacing is increased from 10 to 20 cm, which is mainly due to the substantial channel correlation reduction with the increased PD spacing in the 4×4 MIMO-VLC system.

C. Computational Complexity

Based on the above evaluations, we can see that user-centric aSMP and SD-aSMP greatly outperform conventional SD and SMP, as well as SD/SMP switching. In this section, we analyze the computational complexity of the aSMP and SD-aSMP receivers. Since IM/DD is generally used in typical MIMO-VLC systems, the elements of the MIMO channel matrix are all real values. Here, we only consider the multiplication and the addition of real numbers as operations.

In this article, ZF-based MIMO demultiplexing is adopted due to its simplicity and low complexity. ZF criterion generally requires two matrix multiplications and one matrix inversion. For $N_r \times N_t$ SMP, the matrix multiplication requires $N_t^2 N_r$ real operations and the matrix inversion needs $4N_t^3$ real operations. Therefore, the ZF-based SMP requires a total of $4N_t^3 + 2N_t^2 N_r$ real operations. For $N_r \times N_t$ aSMP or SD-aSMP, according to Algorithms 1 and 2, the total number of real operations is the same, which is obtained by $\sum_{k=1}^{N_t} 4 \ k^3 + 2 \ k^2 N_r$. Since $\sum_{k=1}^{N_t} 4 \ k^3 + 2 \ k^2 N_r < N_t (4N_t^3 + 2N_t^2 N_r)$, the computational complexity of aSMP or SD-aSMP is on the same order as conventional SMP when N_t is not very large. Therefore, the proposed user-centric MIMO techniques can be successfully implemented in practical VLC systems with only slightly increased computational complexity.

TABLE II FEEDBACK REOUIREMENT

User-centric MIMO techniques	Number of feedback bits
SD/SMP switching Adaptive SMP SD-aided adaptive SMP	$\begin{matrix} 1 \\ N_t \\ N_t + \lceil \log_2 N_t \rceil \end{matrix}$

D. Feedback Requirement

In order to successfully implement the proposed user-centric MIMO techniques, a certain amount of feedback information via the uplink transmission is required to adaptively control the ceiling LEDs. The uplink channel can be either a Wi-Fi channel or an infrared channel [6]. Table II lists the number of required feedback bits of three user-centric MIMO techniques. For SD/SMP switching, all the LEDs are working in the same mode, which is either SD or SMP. Hence, only 1 bit feedback information is required for adaptive mode switching [42]. For aSMP, each LED will have two working modes. In the first mode, the LED is driven by both the dc bias and the ac signal for simultaneous lighting and communication. In the second mode, the LED is driven by the dc bias for illumination only. To individually control the working mode of each LED in an indoor $N_r \times N_t$ MIMO-VLC system, a total number of N_t feedback bits is required. However, for SD-aSMP, two parts of feedback information are required. The first part is to individually control the working mode of each LED, which requires N_t feedback bits. The second part is to indicate the index of a specific LED in the LED subset used to transmit independent data streams, which is the farthest from the user, since the rest of LEDs, which are not in the subset, transmit the same data stream as this specific LED. In order to do so, a number of $\lceil \log_2 N_t \rceil$ feedback bits is required, where $\lceil \cdot \rceil$ is the ceiling operator, which outputs an integer larger or equal to its input value. Hence, a total of $N_t + \lceil \log_2 N_t \rceil$ feedback bits are required for SD-aSMP. It can be concluded from Table II that the required feedback information for implementing the proposed user-centric MIMO techniques is quite limited.

E. Feasibility Discussions

The substantial achievable rate improvement of user-centric MIMO techniques over conventional ones is achieved by fully exploiting users' spatial positions as a new degree of diversity, which requires adaptive control of the inputs of different LED transmitters according to the spatial position of the user. Due to user mobility in practical indoor environments, users' spatial positions might be changing with time. In consequence, it is necessary to discuss the feasibility of applying user-centric MIMO techniques in practical VLC systems with mobile users.

To achieve dynamic MIMO mode selection as in SD/SMP switching and dynamic LED subset selection as in aSMP or SD-aSMP, the channel state information (CSI) of a MIMO-VLC system should be first obtained. For efficient CSI estimation, a time-multiplexed training approach can be employed in MIMO-VLC systems [43]. It should be noted that user-centric MIMO techniques require the same signal overhead for CSI estimation as the conventional ones.

It has been shown by [44] that typical VLC systems within a dynamic indoor environment can achieve robust performance and offer excellent mobility even for high user density. Based on these practical measurements, it is believed that VLC systems applying user-centric MIMO techniques can also achieve stable performance. Moreover, indoor users are normally located at some fixed positions or moving with a relatively slow speed, suggesting a relative low speed of channel change. As a result, the frequency of updating feedback information is not high and the uplink delay should have negligible impact on the performance of user-centric MIMO enhanced VLC systems, and hence the proposed user-centric MIMO techniques can be applied to VLC systems with mobile users. To support multiple users, orthogonal frequency division multiple access can be adopted where each user will be allocated with a group of subcarriers, i.e., a sub-band from the overall bandwidth, and user-centric MIMO techniques can be applied within the allocated sub-band of each user without interuser-intereference due to the orthogonality of different sub-bands.

VI. CONCLUSION

In this article, we have proposed and investigated three usercentric MIMO techniques for achievable rate improvement of indoor VLC systems, including SD/SMP switching, aSMP, and SD-aSMP. Compared to conventional MIMO techniques such as SD and SMP, the proposed user-centric MIMO techniques treat the users spatial positions as a new degree of diversity and fully exploit the achievable rate by selecting an optimal working mode for each LED in the MIMO-VLC system. For both aSMP and SD-aSMP, two algorithms for optimal LED subset selection have been developed. We have derived the achievable rates of both conventional and user-centric MIMO techniques with regard to the transmit SNR. It is shown by the detailed simulation results that, in an indoor 4×4 MIMO-VLC system, the achievable rate can be significantly improved by applying the proposed user-centric MIMO techniques compared to the conventional ones. Moreover, the impact of various transmit SNR conditions and geometric setups on the achievable rate of user-centric MIMO-based VLC systems has also been evaluated. Besides, based on our analysis of the computational complexity, it is verified that user-centric MIMO outperforms conventional MIMO under the condition of slightly increased computational complexity with limited feedback information. In summary, this article presents a comprehensive investigation on our proposed user-centric MIMO techniques and the obtained results demonstrate their feasibility and advantages in practical MIMO-VLC systems. In our future work, the bit error rate performance of user-centric MIMO-VLC systems in experiments will be further investigated.

REFERENCES

[1] T. Baumgartner *et al.*, "Lighting the way: Perspectives on the global lighting market," McKinsey Co., Nashua, NH, USA, Tech. Rep., 2012. [Online]. Available: http://www.ledsmagazine.com/articles/2011/08/mckinseyreleases-lightingmarket-report.html

- [2] T. Komine and M. Nakagawa, "Fundamental analysis for visible-light communication system using LED lights," *IEEE Trans. Consum. Electron.*, vol. 50, no. 1, pp. 100–107, Feb. 2004.
- [3] S. Arnon, Visible Light Communication. Cambridge, U.K.: Cambridge Univ. Press, Mar. 2015.
- [4] H. Haas, L. Yin, Y. Wang, and C. Chen, "What is LiFi?" J. Lightw. Technol., vol. 34, no. 6, pp. 1533–1544, Mar. 2016.
- [5] L. Grobe *et al.*, "High-speed visible light communication systems," *IEEE Commun. Mag.*, vol. 51, no. 12, pp. 60–66, Dec. 2013.
- [6] H. Haas, "Visible light communication," in Proc. Opt. Fiber Commun. Conf., Mar. 2015, Paper Tu2G.5.
- [7] H. Le Minh et al., "100-Mb/s NRZ visible light communications using a postequalized white LED," *IEEE Photon. Technol. Lett.*, vol. 21, no. 15, pp. 1063–1065, Aug. 2009.
- [8] D. Tsonev et al., "A 3-Gb/s single-LED OFDM-based wireless VLC link using a Gallium Nitride μLED," IEEE Photon. Technol. Lett., vol. 26, no. 7, pp. 637–640, Apr. 2014.
- [9] S. Rajbhandari et al., "High-speed integrated visible light communication system: Device constraints and design considerations," *IEEE J. Sel. Areas Commun.*, vol. 33, no. 9, pp. 1750–1757, Sep. 2015.
- [10] Y.-F. Liu, Y. C. Chang, C.-W. Chow, and C.-H. Yeh, "Equalization and pre-distorted schemes for increasing data rate in in-door visible light communication system," in *Proc. Opt. Fiber Commun. Conf.*, Mar. 2011, Paper JWA083.
- [11] C. Chen, W.-D. Zhong, and D. Wu, "Indoor OFDM visible light communications employing adaptive digital pre-frequency domain equalization," in *Proc. Conf. Lasers Electro-Opt.*, Jun. 2016, Paper JTh2A.118.
- [12] M. Z. Afgani, H. Haas, H. Elgala, and D. Knipp, "Visible light communication using OFDM," in *Proc. Int. Conf. Testbeds Res. Infrastructures Development Netw. Communities*, Mar. 2006, pp. 129–134.
- [13] K. Akande and W. Popoola, "Spatial carrierless amplitude and phase modulation technique for visible light communication systems," *IEEE Syst. J.*, vol. 13, no. 3, pp. 2344–2353, Sep. 2019.
- [14] H. Marshoud, V. M. Kapinas, G. K. Karagiannidis, and S. Muhaidat, "Non-orthogonal multiple access for visible light communications," *IEEE Photon. Technol. Lett*, vol. 28, no. 1, pp. 51–54, Jan. 2016.
- [15] H. Marshoud, P. C. Sofotasios, S. Muhaidat, G. K. Karagiannidis, and B. S. Sharif, "Error performance of NOMA VLC systems," in *Proc. IEEE Int. Conf. Commun.*, May 2017, pp. 1–6.
- [16] V. K. Papanikolaou, P. D. Diamantoulakis, and G. K. Karagiannidis, "User grouping for hybrid VLC/RF networks with noma: A coalitional game approach," *IEEE Access*, vol. 7, pp. 103299–103309, 2019.
- [17] L. Zeng et al., "High data rate multiple input multiple output (MIMO) optical wireless communications using white LED lighting," IEEE J. Sel. Areas Commun., vol. 27, no. 9, pp. 1654–1662, Dec. 2009.
- [18] C. Chen, W.-D. Zhong, and D. Wu, "On the coverage of multiple-input multiple-output visible light communications [Invited]," *J. Opt. Commun. Netw.*, vol. 9, no. 9, pp. D31–D41, Sep. 2017.
- [19] A. H. Azhar, T. Tran, and D. O'Brien, "A gigabit/s indoor wireless transmission using MIMO-OFDM visible-light communications," *IEEE Photon. Technol. Lett.*, vol. 25, no. 2, pp. 171–174, Jan. 2013.
- [20] C. Chen, W.-D. Zhong, H. Yang, and P. Du, "On the performance of MIMO-NOMA-based visible light communication systems," *IEEE Pho*ton. Technol. Lett., vol. 30, no. 4, pp. 307–310, Feb. 2018.
- [21] T. Fath and H. Haas, "Performance comparison of MIMO techniques for optical wireless communications in indoor environments," *IEEE Trans. Commun.*, vol. 61, no. 2, pp. 733–742, Feb. 2013.
- [22] A. Burton, H. Minh, Z. Ghassemlooy, E. Bentley, and C. Botella, "Experimental demonstration of 50-Mb/s visible light communications using 4 × 4 MIMO," *IEEE Photon. Technol. Lett.*, vol. 26, no. 9, pp. 945–948, May 2014.
- [23] R. Mesleh, H. Elgala, and H. Haas, "Optical spatial modulation," J. Opt. Commun. Netw., vol. 3, no. 3, pp. 234–244, Mar. 2011.
- [24] A. Nuwanpriya, S.-W. Ho, and C. S. Chen, "Indoor MIMO visible light communications: Novel angle diversity receivers for mobile users," *IEEE J. Sel. Areas Commun.*, vol. 33, no. 9, pp. 1780–1792, Sep. 2015.
- [25] T. Chen, Z. Zheng, L. Liu, and W. Hu, "High-diversity space division multiplexing visible light communication utilizing a fisheye-lens-based imaging receiver," in *Proc. Opt. Fiber Commun. Conf.*, Mar. 2015, Paper Tu2G.3.
- [26] C. Chen, W.-D. Zhong, D. Wu, and Z. Ghassemlooy, "Wide-FOV and high-gain imaging angle diversity receiver for indoor SDM-VLC systems," *IEEE Photon. Technol. Lett.*, vol. 28, no. 19, pp. 2078–2081, Oct. 2016.

- [27] C. Chen, W.-D. Zhong, and D. Wu, "Communication coverage improvement of indoor SDM-VLC system using NHS-OFDM with a modified imaging receiver," in *Proc. IEEE Int. Conf. Commun. Workshops*, May 2016, pp. 315–320.
- [28] C. Chen, W.-D. Zhong, and D. Wu, "Non-Hermitian symmetry orthogonal frequency division multiplexing for multiple-input multiple-output visible light communications," J. Opt. Commun. Netw., vol. 9, no. 1, pp. 36–44, Jan. 2017.
- [29] K. Ying, H. Qian, R. J. Baxley, and S. Yao, "Joint optimization of precoder and equalizer in MIMO VLC systems," *IEEE J. Sel. Areas Commun.*, vol. 33, no. 9, pp. 1949–1958, Sep. 2015.
- [30] K. Ying, H. Qian, R. J. Baxley, and G. T. Zhou, "MIMO transceiver design in dynamic-range-limited VLC systems," *IEEE Photon. Technol. Lett.*, vol. 28, no. 22, pp. 2593–2596, Nov. 2016.
- [31] G. Stepniak, J. Siuzdak, and P. Zwierko, "Compensation of a VLC phosphorescent white LED nonlinearity by means of Volterra DFE," *IEEE Photon. Technol. Lett.*, vol. 25, no. 16, pp. 1597–1600, Aug. 2013.
- [32] M. Ijaz et al., "Experimental proof-of-concept of optical spatial modulation OFDM using micro LEDs," in Proc. IEEE Int. Conf. Commun. Workshops, Jun. 2015, pp. 1338–1343.
- [33] X. Zhu, Z. Wang, Q. Wang, and H. Haas, "Virtual spatial modulation for MIMO systems," in *Proc. IEEE Global Commun. Conf.*, Dec. 2016, pp. 1–6.
- [34] P. Deng and M. Kaverhad, "Software defined adaptive MIMO visible light communications after an obstruction," in *Proc. Opt. Fiber Commun. Conf.*, Mar. 2017, Paper Th1E.5.
- [35] O. Narmanlioglu, R. C. Kizilirmak, T. Baykas, and M. Uysal, "Link adaptation for MIMO OFDM visible light communication systems," *IEEE Access*, vol. 5, pp. 26006–26014, 2017.
- [36] X. Bao, X. Gu, W. Zhang, and H.-H. Chen, "User-centric quality-of-experience optimization and scheduling of multicolor LEDs in VLC systems," *IEEE Syst. J.*, vol. 13, no. 3, pp. 2275–2284, Sep. 2019.

- [37] B. W. Kim, "Suboptimal LED selection for distributed MIMO visible light communications," *Pers. Ubiquit. Comput.*, vol. 22, no. 1, pp. 105–110, Feb. 2018.
- [38] C. Chen, W.-D. Zhong, H. Yang, S. Zhang, and P. Du, "Reduction of SINR fluctuation in indoor multi-cell VLC systems using optimized angle diversity receiver," *J. Lightw. Technol.*, vol. 36, no. 17, pp. 3603–3610, Sep. 2018.
- [39] J. Grubor, S. Randel, K.-D. Langer, and J. W. Walewski, "Broadband information broadcasting using LED-based interior lighting," *J. Lightw. Technol.*, vol. 26, no. 24, pp. 3883–3892, Dec. 2008.
- [40] P. Djahani and J. M. Kahn, "Analysis of infrared wireless links employing multibeam transmitters and imaging diversity receivers," *IEEE Trans. Commun.*, vol. 48, no. 12, pp. 2077–2088, Dec. 2000.
- [41] Lighting of Indoor Work Places, European Standard EN 12464-1, Jan. 2009.
- [42] X. Guo, X. Li, and R. Huang, "Adaptive multiple-input multiple-output mode switching for indoor visible light communication system with orthogonal frequency division multiplexing modulation," *Chin. Opt. Lett.*, vol. 15, no. 11, Nov. 2017, Art. no. 110604.
- [43] Y. Wang and N. Chi, "Demonstration of high-speed 2 × 2 non-imaging MIMO Nyquist single carrier visible light communication with frequency domain equalization," *J. Lightw. Technol.*, vol. 32, no. 11, pp. 2087–2093, Jun. 2014
- [44] P. Chvojka, S. Zvanovec, P. A. Haigh, and Z. Ghassemlooy, "Channel characteristics of visible light communications within dynamic indoor environment," *J. Lightw. Technol.*, vol. 33, no. 9, pp. 1719–1725, May 2015.